Earth Sciences
2018; 7(4): 166-174
http://www.sciencepublishinggroup.com/j/earth
doi: 10.11648/j.earth.20180704.14
ISSN: 2328-5974 (Print); ISSN: 2328-5982 (Online)

Numerical Simulation of Diagenetic Stage in Sandstone Reservoir of Huagang Formation in Xihu Sag

Xia Min[1], Yin Taiju[2, *], Qian Wendao[2], Zhang Changmin[2], Hou Guowei[3], He Miao[3]

[1]College of Resources and Environment of Yangtze University, Wuhan, China

[2]School of Geoscience of Yangtze University, Wuhan, China

[3]Shanghai Branch of CNOOC Ltd., Shanghai, China

Email address:

736519400@qq.com (Xia Min), yintaij@yangtzeu.edu.cn (Yin Taiju), 932408129@qq.com (Qian Wendao), zcm@yangtzeu.edu.cn (Zhang Changmin), hougw@cnooc.com.cn (Hou Guowei), 905665922@qq.com (He Miao)

[*]Corresponding author

To cite this article:

Xia Min, Yin Taiju, Qian Wendao, Zhang Changmin, Hou Guowei, He Miao. Numerical Simulation of Diagenetic Stage in Sandstone Reservoir of Huagang Formation in Xihu Sag. *Earth Sciences*. Vol. 7, No. 4, 2018, pp. 166-174. doi: 10.11648/j.earth.20180704.14

Received: June 20, 2018; **Accepted**: July 3, 2018; **Published**: July 27, 2018

Abstract: To predict distribution of diagenetic stages of Xihu Sag Huagang Formation sandstone reservoir and secondary pore development zone, and research original pore reservation and secondary pore increase and decrease in reservoir evolution process, combining traditional diagenesis research and numerical simulation technique, and based on interaction model and effect model, this paper establishes a aggregative model on numerical simulation of diagenetic stages. In diagenesis simulation process, based on process response principle, and restricted by current diagenetic stage distribution and type, diagenetic stage distribution and type of reservoir during geological historical evolution period is back stripped through diagenetic temperature. Taking single well diagenetic stage data as constraint condition, and combining with research area burial history, ground temperature history, and diagenetic stage division basis, and scheme, plane distribution of diagenetic stages of the whole research area during each geological historical period is finally obtained.

Keywords: Xihu Sag, Diagenesis, Diagenetic Stage, Numerical Simulation

1. Introduction

The evolution of reservoirs pore is mainly controlled by diagenesis and sedimentary facies, where sedimentary facies affects pore evolution at shallow and deep buried depth, respectively [1-3]. As an essential process for the generation and development of all kinds of reservoirs, diagenesis fundamentally determines the physical property of all reservoirs, which is especially true for low-porous and low-permeable reservoir [4-6].

Clastic rock diagenetic stage represents different geological historical evolution stages experienced by clastic sediment under all kinds of diagenesis transformation after deposition to the period before metamorphism [7]. Whether hydrocarbon source rock generates hydrocarbon is closely concerned with diagenetic stages, and post mature hydrocarbon source rock (Ro>1.3%) is generally unbeneficial to oil gas generation, and therefore, research on diagenetic stages of research area contributes to beneficial oil-gas exploration area finding [8, 9]. Diagenetic stage of clastic sediment in burial stage is closely concerned with oil and gas accumulation property of clastic pore development and evolution to reservoir stratum.

Diagenesis and pore evolution not only affect pore formation, increase and decrease of oil and gas reservoir stratum, but also affect primary pore preservation, secondary pore distribution and pore connection and penetration property. Therefore, diagenesis and pore evolution have basic effect on quality of reservoir, and in research on diagenesis of reservoir, it is necessary to divide diagenesis stage and pore evolution stage of research area.

2. Geology

Xihu Sag sits in the shelf basin in the northeast of East Sea, distributed in direction of NNE. It is connected with Hupijiao

Reef, Haijiao Reef, and Yushan Uplift in west, and adjacent to Diaoyu Island magmatic rock zone in east, and respectively transits to Fujiang depression and Jilong depression through a high saddle in north and south (Figure 1). Xihu Sag is generally a structural pattern of "two depressions and one uplift", and has structural feature of "east-west zoning and south-north blocking".

According to Cenozoic structural pattern, depositional feature, fault development and the characteristics of oil gas etc., Xihu Sag is classified into 3 secondary structural units, i.e. west gentle slope (slope) belt, central depression-inverted structure belt and east continental slope fault-uplift belt [10, 11], from west to east, where, central depression-inverted structure belt includes east sub-depression, central inverted structure belt and west sub-depression from east to west, and central inverted structure belt can be further divided into Jiaxing structure belt, Ningbo structure belt, Huangyan structure belt, Tiantai structure belt and Jilong structure belt from north to south.

From the bottom to the top, the Xihu Sag develops the formation of Eocene Bajiaoting and Pinghu, Oligocene Huagang, Miocene Longjing, Yuquan, and Liulang, Pliocene Santan formation and Pleistocene the East China Sea group etc. Oligocene Huagang formation is one of the main target formations at present, and can be divided into Hua upper section (H1—H4) and Hua lower section (H5—H8) from the top to the bottom.

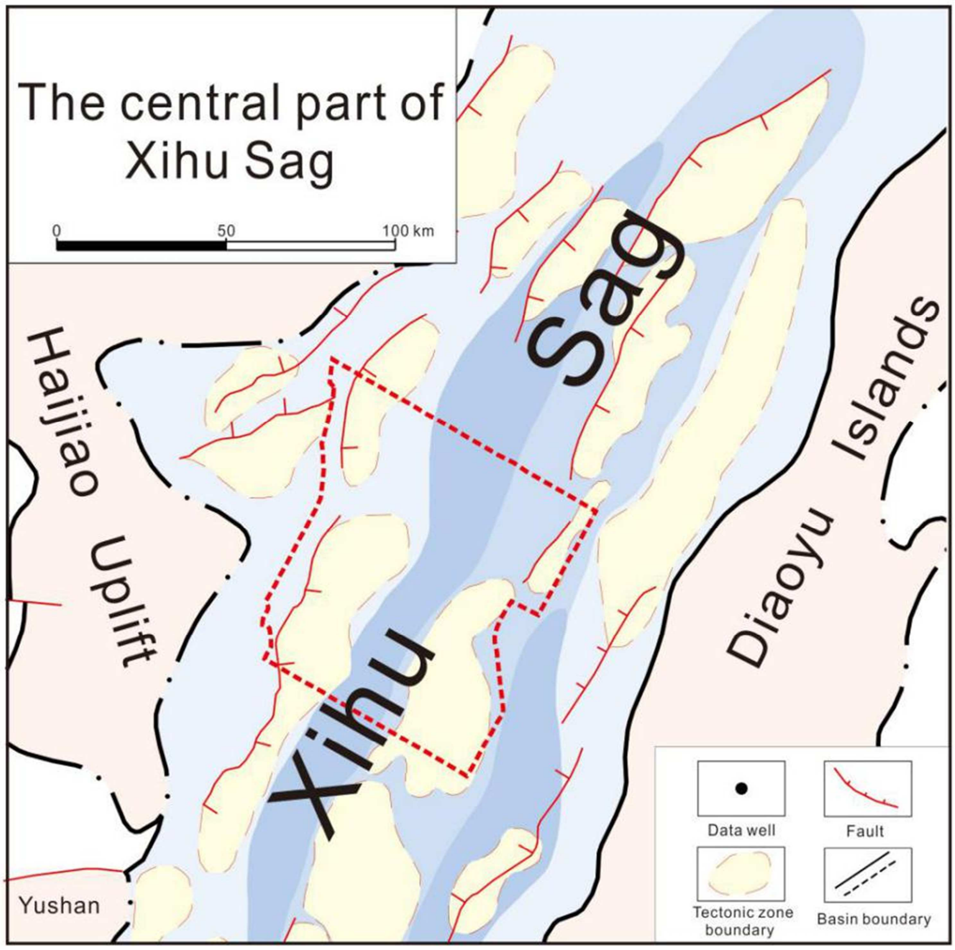

Figure 1. *Location and tectonic setting of study area.*

3. Diagenetic Stage Simulation Principle

Process response principle is basic scientific principle. Response characteristic depends on effect process. The reservoir is common result of sedimentary, diagenetic and tectonic action in geological history. Considering all kinds of geologic process to reservoir during different periods, especially the condition difference in geologic process at different periods, and effect result of these differential geological conditions, good means can be provided for prediction to reservoir at high diagenetic stage [12].

In diagenesis simulation process, restricted by current diagenetic stage distribution and type, diagenetic stage distribution and type of reservoir during geological historical evolution period is back stripped through diagenetic temperature. Taking single well diagenetic stage data as constraint condition, and combining with research area burial history, ground temperature history, and diagenetic stage division basis, and scheme, plane distribution diagram of diagenetic stages of the whole research area can be obtained [13, 14].

4. Diagenetic Stage Division and Parameter Analysis

4.1. Diagenetic Stage Division Basis

Main basis of current clastic rock diagenetic stage division and research of China is Specification for Oil and Gas Industry Standard Clastic Rock Diagenetic Stage Division of the People's Republic of China, and main parameters on diagenetic stage division in the specification includes: (1) paleogeo temperature, (2) maturity of organic matter, (3) clay mineral evolution, (4) distribution and formation sequence of authigenic mineral in sandstone, (5) rock structure, construction features and pore type etc.

Clay mineral is mineral widely existing in clastic rocks, and it is generally considered that in diagenesis research, clay mineral combination and clay mineral mixed-layer ratio size, I/S mixed layer clay mineral evolution and organic matter evolution maturity are main basis on diagenetic stage division, and make diagenesis research developed from qualitative research to quantitative research. According to new diagenetic stage division standard (No. SY/T5477-2003) in oil and gas industry of the People's Republic of China (Table 1), diagenetic stages are classified according to percentage composition of smectite in clay mineral I/S and vitrinite reflectance (Ro) characteristics, with thermal maturity of organic matter and clay mineral adopted as main indexes.

Table 1. *Division of diagenesis stages in clastic rocks.*

Diagenetic Stage (DS-i)	Paleo Temperature (°C)	Organic	Mudstone
		Vitrinite Reflectance (Ro)	I/S-S%
DS-IA	≤65	＜0.35	>70
DS- IB	>65~85	0.35~0.55	70~50
DS-IIA1	>85~110	0.55~0.7	50~20
DS-IIA2	>110~140	0.7~1.3	20~15
DS-IIB	>140~175	1.3~2.0	＜15
DS-III	>175	>2.0	~

4.2. Vitrinite Reflectance Analysis

Seen from Ro test data of partial wells of research area, Ro value of most wells is 0.60%-0.85% (Table 2), and with increase of burial depth, Ro value presents increase tendency, and organic matter maturity is at low mature - mature stage, being at middle diagenetic stage A.

Table 2. *Partial well drilling Ro values in Xihu Sag.*

Well name	Ro, max (%)	Ro, ave (%)
HY7-3-1	0.815	0.766
NB17-1-2	0.819	0.816
PH11	0.840	0.750
NB17-1-3	0.858	0.849
NB27-5-4	0.758	0.75

4.3. Analysis on Relative Content of Clay Minerals of Reservoir

According to diagenetic stage division standard, in illite / smectite mixed-layer, content of smectite (%S) ＜15% is the sign for entry into middle diagenetic stage B (Figure 2). Diagenetic evolution experienced by Huagang formation reservoir of each tectonic region of Xihu Sag does not exceed scope of middle diagenetic stage, and is dominated by middle diagenetic stage A.

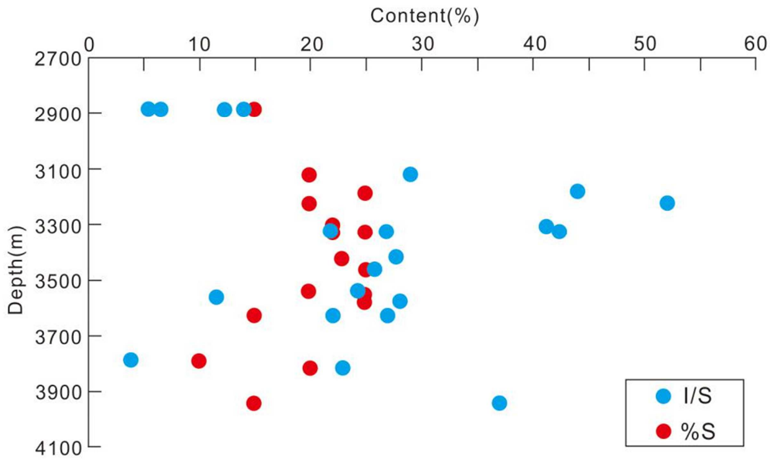

Figure 2. *Determination of Relative Content of Clay Minerals in Huagang Formation.*

4.4. Analysis on Maximum Temperature of Thermolysis

According to diagenetic stage division standard, when maximum temperatures of thermolysis (Tmax) in thermal evolution process of organic matter is greater than 490°C, rock starts to enter into late diagenetic stage.

Seen from test data, maximum temperatures of thermolysis (Tmax) displayed in reservoir rock thermolysis analysis data of Xihu Sag is between 431°C—479°C (Table 3). According to diagenetic stage division standard of oil and gas industry of China in 2003, it is determined that Huagang formation reservoir sandstone of each block of Xihu Sag is totally at the stage of middle diagenetic, and no reference about the late diagenetic stage evidence is found.

Table 3. Reservoir rock pyrolysis analysis data in Xihu Sag.

Well name	Tmax (°C)		
	Min	Max	Ave
NB17-1-4	403	467	433.5
NB22-1-1	464	470	467
NB27-1-2	415	479	458.2
HY2-2-1	421	454	445.2
NB27-5-4	406	469	453.9

Through comprehensive analysis to evolution characteristics and diagenetic evolution sequence of hydrocarbon source rock of each block of Xihu Sag, diagenetic change of Huagang formation is divided into 3 stages and 4 stage times, i.e. syndiagenetic stage, early diagenetic stage A and B, and middle diagenetic stage A and B.

Although current diagenetic stage of north central part and south central part of central inverted structure belt deviates from diagenetic environment in a certain degree, there is no big difference in overall evolution process [15]. Therefore, combining with predecessor's research, it is considered that diagenetic sequence and diagenetic environment of Xihu Sag Huagang formation reservoir sandstone in overall evolution process successively experience [16]: alkalescence of early diagenetic stage A →weak acidity of early diagenetic stage B →acidity of middle diagenetic stage A—acid-base transition belt →alkalinity of middle diagenetic stage B.

5. Diagenetic Stage Simulation

5.1. Single Well Diagenetic Stage

Based on basic cognition to overall evolution route of diagenetic sequence and diagenetic environment of reservoir sandstone of research area, vertical division research aimed at diagenetic sequence and diagenetic environment of typical drilling of each main tectonic region within depression is further developed. Select well NB27-5-2 of research area located in west sub-depression for illustration (Figure 3).

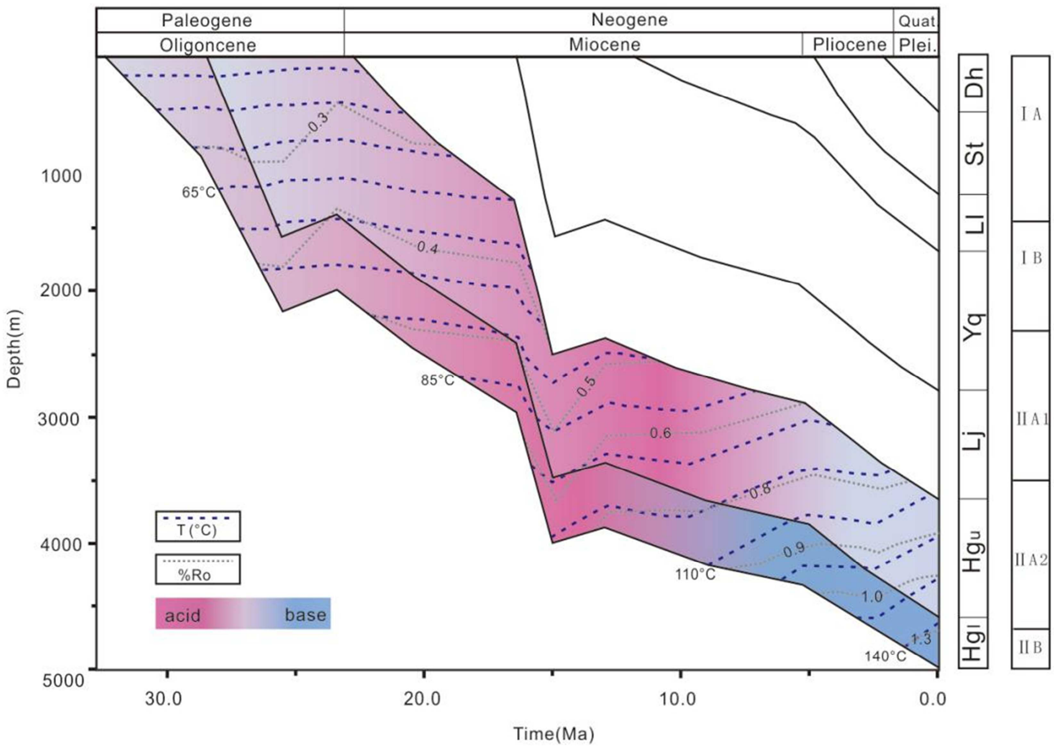

Figure 3. NB27-5-2 buried history and vertical division of diagenetic environment.

Upper part of Liulang formation of well NB27-5-2 of west sub-depression and shallow layer (＜1400m), alkalescence diagenetic environment, according to burial-thermal history: Ro＜0.35%, early rimmed chlorite, at early diagenetic stage A.

Upper part of Yuquan formation to lower part of Liulang formation (1400m—2300m), faintly acid diagenetic environment, according to burial-thermal history: 0.35%＜Ro ＜ 0.5%, stage 1 acidity dissolution, early calcite cementing starting, point contact, quartz level-I secondary enlargement (autogenic kaolinite may begin to be developed), at early diagenetic stage B.

Lower part of Longjing formation to middle part of Yuquan formation (2300m—3500m), acidity diagenetic environment, according to burial-thermal history: 0.5%<Ro<0.7%, acidity dissolution may last, line contact, quartz level-II secondary enlargement, at middle diagenetic stage A1.

Huagang formation H6 single layer to lower part of Longjing formation (3500m—4700m), acid-base transition belt, according to burial-thermal history: 0.7%<Ro<1.3%, kaolinite disappearance, acicular illite, late-stage iron carbonate cementing, quartz level-III secondary enlargement, concave and convex - line contact, quartz dissolution, measured smectite content in illite / smectite mixed-layer is 15%—20%, and relative average content of kaolinite is 5.75%, at middle diagenetic stage A2.

Huagang formation H7 single layer to H9 single layer (>4700m), alkalinity diagenetic environment, according to burial-thermal history: 1.3% < Ro, late iron carbonate cementing development, hair-shaped illite, quartz level-III secondary enlargement, line- concave and convex contact, pore nondevelopment, measured smectite content in illite / smectite mixed-layer is 15%, and relative average content of kaolinite is 6.41%, at middle diagenetic stage B.

Vertical evolutionary analysis on diagenetic stage division and diagenetic environment of typical well at each tectonic division of research area shows: middle diagenetic stage A1 has relatively strong acidity diagenetic environment, and Huagang formation at the diagenetic stage has good secondary dissolved pore development; middle diagenetic stage A2 has acid-base transition belt diagenetic environment, and Huagang formation at the diagenetic stage has weakened dissolution effect and enhanced cementing with decrease of reservoir physical property; middle diagenetic stage B is facing alkalinity diagenetic environment, and the main diagenesis of Huagang formation at the diagenetic stage is compaction and cementing, and affected by this, its reservoir has the worst level. The research considers that lower limit of beneficial diagenetic facies band in vertical direction is basically equivalent to bottom margin of middle diagenetic stage A2 (Figure 4).

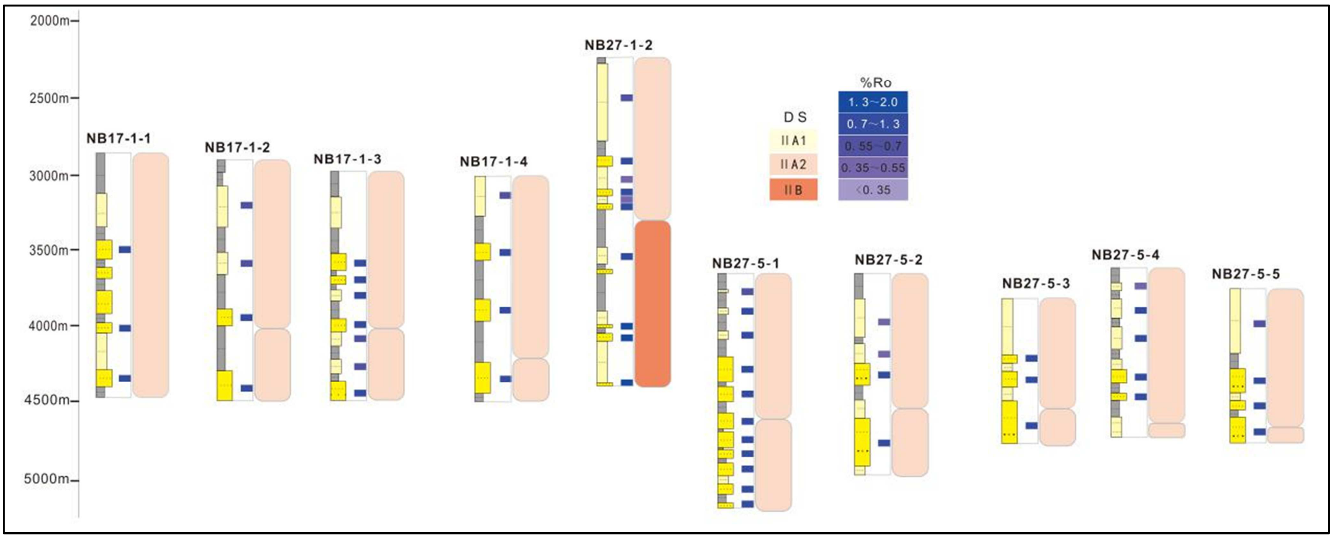

Figure 4. *Single well diagenetic stage.*

5.2. Diagenetic Stages of Area

5.2.1. Evolution Stage Time Determination

Evolution stage experienced by target layer during geological historical period is divided according to development of overlying formation of target layer. Assumed that target layer L has i layers of overlying formation, which means that overlying formation is marked as follows from the top to the bottom: L1, L2, L3……Li-1 and Li, then target layer has i evolution stages in total during geological historical period, and according to time evolution, and sequential order of evolution stage time of target layer L successively is Li, Li-1, Li-2……L2, L1. From the bottom to the top, overlying formation of Huagang formation of research area respectively is Longjing formation, Yuquan formation, Liulang formation, Santan formation and shallow layer, so Huagang formation has 4 evolution stages in total during geological historical period.

5.2.2. Determination to Burial Depth of Different Stage Time

Based on last step, burial depth of target layer L during different evolution periods is calculated and its computational formula is as follows:

$$\begin{aligned} \text{Dep (Li)} &= \text{H (L)} - \text{H (Li)}; \\ \text{Dep (Li} - 1) &= \text{H (L)} - \text{H (Li} - 1); \\ \text{Dep (Li} - 2) &= \text{H (L)} - \text{H (Li} - 2); \\ &\cdots\cdots \\ \text{Dep (L2)} &= \text{H (L)} - \text{H (L2)}; \\ \text{Dep (L1)} &= \text{H (L)} - \text{H (L1)}; \end{aligned} \tag{1}$$

Where: H (L) is top interface of target layer L, H (Li) is top interface of overlying formation Li, and Dep (Li) is stage burial depth of target layer Li; (Figure 5).

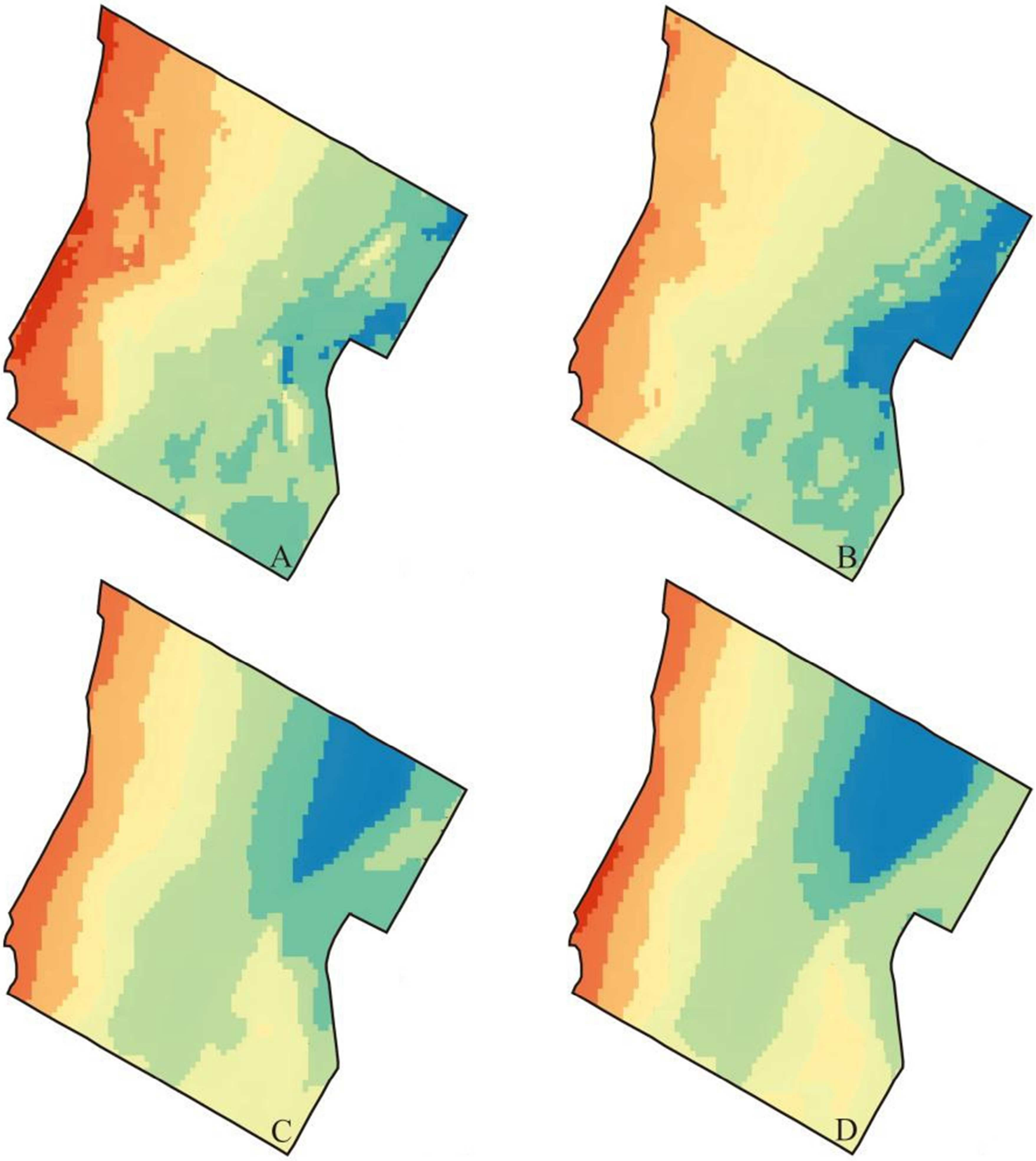

Figure 5. *Huagang Formation buried depth evolution plans. (A) The buried depth plan of the Longjing Formation after deposition; (B) The buried depth plan of the Yuquan Formation after deposition; (C)The buried depth plan of the Liulang Formation after deposition; (D) The buried depth plan of the Santan Formation after deposition.*

5.2.3. Determination to Formation Temperature of Different Stage Time

In burial process of geologic body, temperature level is expressed as a linear function relationship with depth, and through following temperature calculation model, formation temperature of target layer L at different periods, different depth and different position is calculated; temperature calculation model formula [17, 18]:

$$T=T0+c*(Dep\ (Ti)-H0) \quad (2)$$

Where, T0 is temperature of normal temperature belt, c is constant, Dep (Ti) is stage burial depth of target layer Ti, H0 is burial depth of constant temperature belt, being constant and T is paleogeotemperature of target layer (Figure 6).

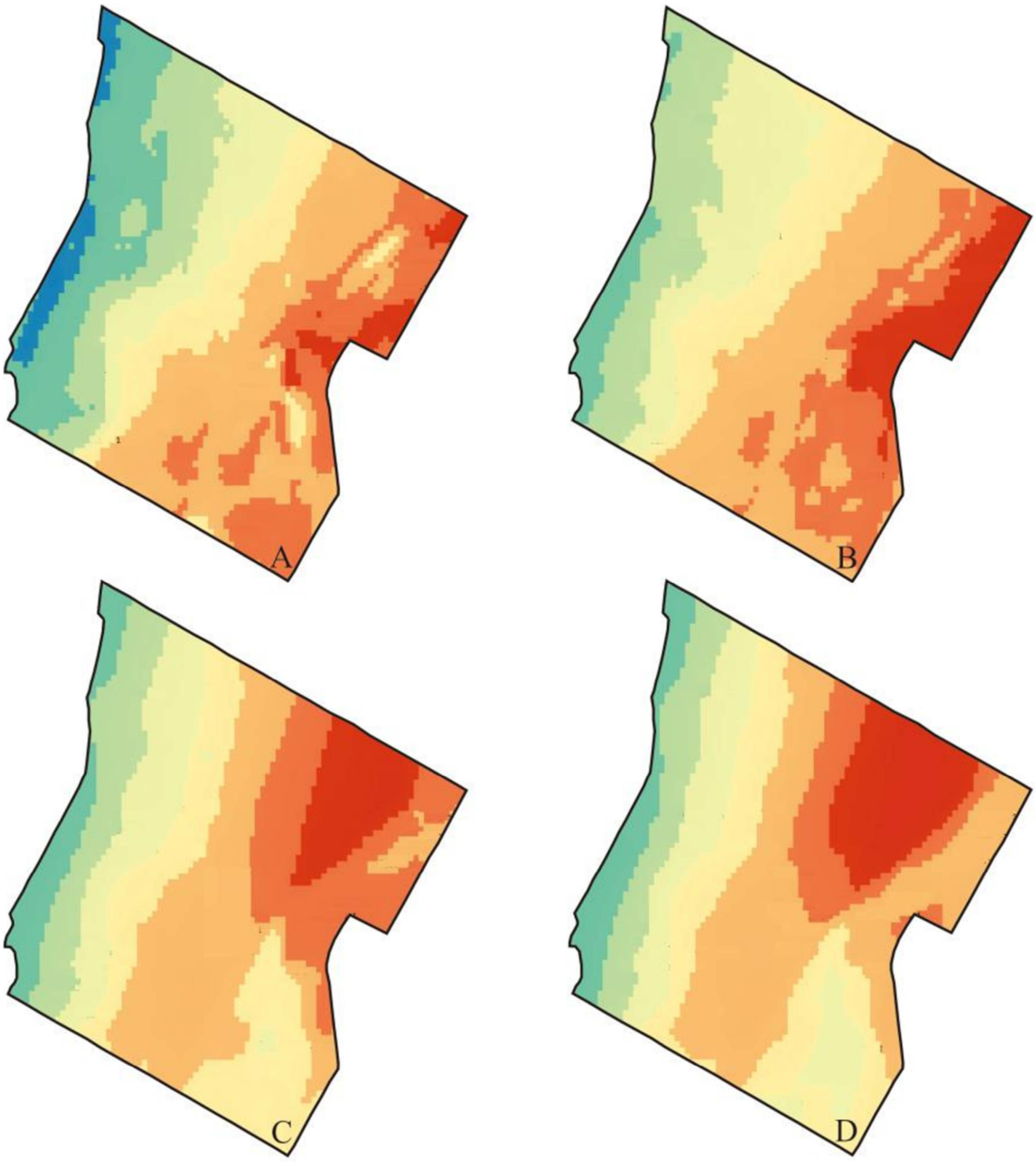

Figure 6. *Huagang Formation paleo temperature evolution plans. (A) The paleo temperature plan of the Longjing Formation after deposition; (B) The paleo temperature plan of the Yuquan Formation after deposition; (C)The paleo temperature plan of the Liulang Formation after deposition; (D) The paleo temperature plan of the Santan Formation after deposition.*

5.2.4. Determination to Diagenetic Stages of Formation of Different Stage Time

When T∈[20~65), DS is early stage of early diagenetic stage, i.e. ⅠA;

When T∈[65~85), DS is late stage of early diagenetic stage, i.e. ⅠB;

When T∈[85~110), DS is early stage 1 of middle diagenetic stage, i.e. ⅡA1;

When T∈[110~140), DS is early stage 2 of middle diagenetic stage, i.e. ⅡA2;

When T∈[140~175), DS is late stage of middle diagenetic stage, i.e. ⅡB;

When T∈[175~200), DS is late diagenetic stage, i.e. III.

Finally, in diagenesis simulation process, restricted by current diagenetic stage distribution and type, diagenetic stage distribution and type of reservoir during geological historical evolution period is back stripped through diagenetic temperature to obtain plane distribution diagram of diagenetic stages of the whole research area during each geological historical period (Figure 7).

After deposition of Longjing formation, Huagang formation comes to early diagenetic stage A and B (Figure 7 A); after deposition of Yuquan formation, Huagang formation comes to early diagenetic stage A - middle diagenetic stage A1(Figure 7 B); after deposition of Liulang formation, Huagang formation comes to middle diagenetic stage B- early diagenetic stage A (Figure 7 C); after deposition of Santan formation, Huagang formation is still at middle diagenetic stage B- early diagenetic stage A (Figure 7 D).

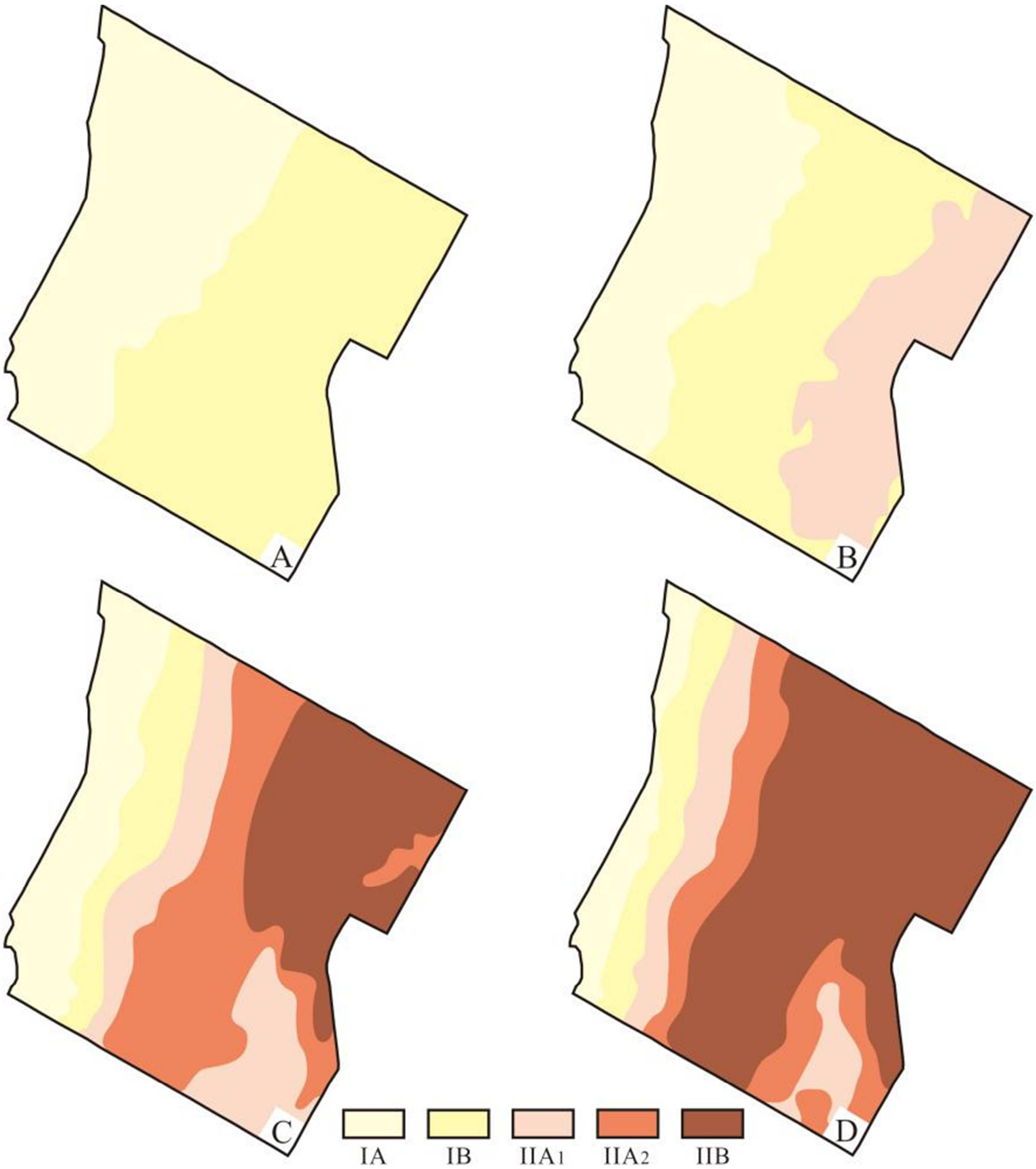

Figure 7. *Huagang Formation diagenetic stage evolution plans. (A) The diagenetic stage plan of the Longjing Formation after deposition; (B) The diagenetic stage plan of the Yuquan Formation after deposition;(C) The diagenetic stage plan of the Liulang Formation after deposition; (D) The diagenetic stage plan of the Santan Formation after deposition.*

6. Conclusions

(1) Diagenetic change of Huagang formation can be divided into three stages and four stage times, i.e. syndiagenetic stage, early diagenetic stage A and B, and middle diagenetic stage A and B. Diagenetic sequence and diagenetic environment of reservoir sandstone in overall evolution process successively experience: alkalescence of early diagenetic stage A →weak acidity of early diagenetic stage B →acidity—acid-base transition belt of middle diagenetic stage A→alkalinity of middle diagenetic stage B.

(2) When Huagang formation occurs at middle diagenetic stage A1, it has good secondary dissolved pore development; Huagang formation at middle diagenetic stage A2 has weakened dissolution effect and enhanced cementing with decrease of reservoir physical property; main diagenesis of Huagang formation at middle diagenetic stage B is compaction and cementing, and affected by this, its reservoir has the worst level. The research considers that lower limit of beneficial diagenetic facies band in vertical direction is basically equivalent to bottom margin of middle diagenetic stage A2.

(3) After deposition of Longjing formation, Huagang formation enters into early diagenetic stage A and B; at the end of Yuquan formation, Huagang formation is at early diagenetic stage A - middle diagenetic stage A1; at the end of Liulang formation, Huagang formation is at middle diagenetic stage B- early diagenetic stage A; at the end of Santan formation, Huagang formation is still at middle diagenetic stage B- early diagenetic stage A.

Acknowledgements

This work received the financial support from Major Projects of National Science and Technology named “Large Oil and Gas Fields and CBM Development”(Grant No. 2016ZX05027). Grateful thanks are given to Shanghai Branch of CNOOC Ltd. for offering us the geological data. Thanks are also given to the reviewers for their valuable advice.

References

[1] Meng Yuanlin, Jiang Wenya, Liu Dela, et al., 2008. Reservoir Porosity Prediction and Its Evolving History Modeling: a case of Shuang qing Region in the Liaohe West Depression. Acta Sedimentologica Sinica, 26(5):780—788.

[2] Zou Caineng, Tao Shizhen, Zhang Xiangxiang, et al., 2009. Differences and Relations between Unconventional and Conventional Oil and Gas. China Petroleum Exploration, 52(8):1068—1090.

[3] Orhan Mahmic, Henning Dypvik, Hammer Erik, 2018. Diagenetic influence on reservoir quality evolution, examples from Triassic conglomerates/arenites in the Edvard Grieg field, Norwegian North Sea. Marine and Petroleum Geology. 93, 247-271.

[4] Michael D. Wilson and Peter T. Stanton, 1994. Diagenetic Mechanisms of porosity and permeability reduction and enhancement. SEPM Short Course, 59—118.

[5] Li Z, Chen J S and Guan P, 2006. Scientific problems and frontiers of sedimentary diagenesis research in oil-gas-bearing basins. Acta Petrologica Sinica, 22(8):2113—2122.

[6] Zhang Shaonan, 2008. Tight sandstone gas reservoirs: their origin and discussion. Oil & Gas Geology, 29(1):1—11.

[7] Xia Min, Yin Taiju, Zhang Changmin, et al., 2017. Characterization and Numerical Simulation of Diagenesis of Clastic Rocks. Bulletin of mineralogy, petrology and geochemistry, 36(suppl.):970—971.

[8] Randolph T. Williams, John R. Farver, Charles M. Onasch, Daniel F. Winslow, 2015. An experimental investigation of the role of microfracture surfaces in controlling quartz precipitation rate: Applications to fault zone diagenesis. Journal of Structural Geology 74 (2015): 24-30.

[9] Guanghui Yuan, Yingchang Cao, Jon Gluyas, Zhenzhen Jia, 2017. Reactive transport modeling of coupled feldspar dissolution and secondary mineral precipitation and its implication for diagenetic interaction in sandstones. Geochimica et Cosmochimica Acta, 207:232–255.

[10] Ye Jiaren, Gu Huirong, Jia Jianyi, 2005. Research on the Hydrocarbon Accumulation Dynamics of Xihu Sag, East China Sea Shelf Basin. Natural Gas Industry, 25(12):5—8.

[11] Zhou Zhiwu, Yin Peiling, 1985. A Geological Review of the East China Sea and its Petroleum potential. Oil & Gas Geology, 6(1):1—14.

[12] Qian Wendao, Yin Taiju, Zhang Changmin, et al., 2017. Forming Condition and Geology Prediction Techniques of Deep Clastic Reservoirs. Acta Geologica Sinica (English Edition), 91(supp. 1):255—256.

[13] Stephan Stricker, Stuart J. Jones, Shanvas Sathar, Leon Bowen, Norman Oxtoby, 2015. Exceptional reservoir quality in HPHT reservoir settings: Examples from the Skagerrak Formation of the Heron Cluster, North Sea, UK. Marine and Petroleum Geology, 77: 198-215.

[14] K. E. Higgs, E. M. Crouch, J. I. Raine, 2016. An interdisciplinary approach to reservoir characterisation; an example from the early to middle Eocene Kaimiro Formation, Taranaki Basin, New Zealand. Marine and Petroleum Geology, 86: 111-139.

[15] Zhang Wu, Xu Fa, Xu Guosheng, et al., 2012. Diagenesis and pore evolution of Huagang Formation tight sandstone reservoirs in a structural belt of Xihu depression in East China Sea Basin. Journal of Chengdu University of Technology (Science & Technology Edition), 39(2):123—129.

[16] Xu Guosheng, Xu Fanggen, Yuan Haifeng, et al., 2016. Evolution of pore and diagenetic environment for the tight sandstone reservoir of Paleogene Huagang Formation in central reversal structural belt in Xihu Sag, East China Sea. Journal of Chengdu University of Technology (Science & Technology Edition), 43(4):385—395.

[17] Zahra Sadat Mashhadi, Ahmad Reza Rabbani, Mohammad Reza Kamali et al., 2015. Burial and thermal maturity modeling of the Middle Cretaceous-Early Miocene petroleum system, Iranian sector of the Persian Gulf. Petroleum Science. 2015(03): 367–390.

[18] Ahmed Awadalla, Omar A. Hegab, Mohammed A. Ahmed, Saad Hassan, 2018. Burial and thermal history simulation of the Abu Rudeis-Sidri oil field, Gulf of Suez-Egypt: A1D basin modeling study. Journal of African Earth Sciences, 138: 86-101.